Published in final edited form as:
J Dermatol Sci. 2007 December ; 48(3): 177–188.

TOPICAL APPLICATION OF LAMININ-322 TO DIABETIC MOUSE WOUNDS

Stephen R. Sullivan, M.D.[++], **Robert A. Underwood, B.F.A.**[†], **Randall O. Sigle, Ph.D.**[*], **Yuko Fukano, M.D.**[†], **Lara A. Muffley, B.S.**[++], **Marcia L. Usui, B.S.**[†], **Nicole S. Gibran, M.D.**[++], **Marcos A. Antezana, M.D.**[†], **William G. Carter, Ph.D.**[*,#], and **John E. Olerud, M.D.**[†]

†*Department of Medicine (Dermatology), University of Washington, Seattle, Washington*

++*Department of Surgery (Plastic and Reconstructive Surgery, University of Washington, Seattle, Washington*

#*Department of Pathobiology, University of Washington, Seattle, Washington*

**Fred Hutchinson Cancer Research Center, Seattle, Washington*

Abstract

Background—Keratinocyte migration is essential for wound healing and diabetic wound keratinocytes migrate poorly. Keratinocyte migration and anchorage appears to be mediated by laminin-332 (LM-332). Impaired diabetic wound healing may be due to defective LM-332 mediated keratinocyte migration.

Objective—To evaluate LM-332 expression in diabetic (db/db) and control (db/-) mice and to test LM-332 wound healing effects when applied to mouse wounds.

Methods—LM-332 expression in mouse wounds was evaluated using immunohistochemistry. LM-332 wound healing effects were evaluated by directly applying soluble LM-332, a LM-332 biomaterial, or a control to mouse wounds. Percent wound closure and histology score, based on healing extent, were measured.

Results—Precursor LM-332 expression was markedly reduced in db/db when compared to db/- mice. *In vitro*, soluble LM-332 and LM-332 biomaterial demonstrated significant keratinocyte adhesion. *In vivo*, soluble LM-332 treated wounds had the highest histology score, but significant differences were not found between wound treatments ($p>0.05$). No differences in percentage wound closure between treatment and control wounds were found ($p>0.05$).

Conclusion—The db/db wounds express less precursor LM-332 when compared to db/-. However, LM-332 application did not improve db/db wound healing. LM-332 purified from keratinocytes was primarily physiologically cleaved LM-332 and may not regulate keratinocyte migration. Application of precursor LM-332 rather than cleaved LM-332 may be necessary to improve wound healing, but this isoform is not currently available in quantities sufficient for testing.

Corresponding author and requests for reprints: John E. Olerud, M.D., Department of Medicine (Dermatology), University of Washington, 1959 NE Pacific St, Box 356524, Seattle, WA 98195-6524, Telephone: (206) 543-5290, Fax: (206) 543-2489, e-mail: olerudje@u.washington.edu.

INTRODUCTION

Chronic, non-healing foot and leg ulcers are the most common cause of lower extremity amputation in patients with diabetes mellitus (1). It is estimated that 15% of individuals with diabetes mellitus will develop lower extremity ulcers (2) and 14 – 24% of diabetic patients with foot ulcers will eventually undergo amputations (3). A better understanding of the pathogenesis of diabetic ulcers and novel treatment strategies are required to reverse the rising rate of amputation.

Genetically diabetic (db/db) mice have been used extensively as a model to study wound healing as it relates to diabetes mellitus and the role of therapeutic topical reagents in wound healing (4-7). The db/db mice have an autosomal recessive mutation that results in defective leptin receptors in the hypothalamus. This defect leads to increased appetite, decreased energy expenditure, obesity and development of marked hyperglycemia that resembles human type 2 diabetes mellitus (8-10). This mouse also demonstrates delayed wound healing (7). Whereas normal murine wounds heal approximately 90% by contraction, db/db mice exhibit less contraction and a much greater degree of epithelization (7), thus serving as a valuable model to study keratinocyte (KC) migration in a diabetic animal following cutaneous injury.

We have demonstrated that in chronic wounds from patients with diabetes mellitus, KCs proliferate at the wound edge, but migrate poorly (11). These results are in agreement with studies of venous ulcers conducted by Andriessen et al. showing that KC at the edges of chronic venous ulcers are highly proliferative (12). Wound margin keratinocyte migration is essential in the epithelization of cutaneous human wounds (13,14). KC migration and anchorage are mediated by laminin-332 (LM-332 previously called laminin 5 or epiligrin). LM-332, a matrix component in the epithelial basement membrane, is expressed by leading KCs migrating at a wound edge and serves as the major adhesive ligand in the basement membrane (15-17). Leading KCs express integrins α6β4, α3β1, α2β1, α5β1 αvβ5, αvβ6, αvβ8 and α9β1 and can adhere to LM-332, collagen, fibronectin, vitronectin, or tenascin in wound repair (18,19). The regulation of KC migration by integrin α3β1 and KC adhesion by integrin α6β4 have been demonstrated (20-23). The role of LM-332 in stable KC adhesion via the integrin α6β4, a component of hemidesmosomes, is documented both in humans (24) and mice (25). However, the role of LM-332 in KC migration with wound closure is controversial. Some studies have shown that LM-332 promotes KC migration (14,15,26,27) while others have shown that LM-332 inhibits KC migration (20,28,29).

LM-332 is a trimer with genetically distinct α3, β3 and γ2 subunits (17,30) (Figure 1). Initially synthesized by wound edge leading KCs as a 460 kDa molecule, uncleaved LM-332 is deposited in the provisional basement membrane of a wound (31). LM-332 contains LG4/5 globular domains at the carboxy terminus (32) that interact with integrin α3β1 to enhance KC migration (14,15,26,33,34). LM-332 undergoes specific physiological post-translational modification of the α3 chain from the precursor 200 kDa chain to the cleaved 165 kDa chain (17,31,35,36). We have noted that very little precursor LM-332 is present at the wound edge in human diabetic ulcers and that mRNA for LM-332 is also absent (37). Our preliminary studies have also shown that LM-332 was greatly reduced in leading edge KCs of diabetic db/db mouse wounds compared to db/- littermates. Since there is considerable evidence that LM-332 plays an important role in KC migration, we wondered whether providing LM-332 to diabetic db/db mouse wounds would restore normal KC migration across the wound surface. The purpose of our study was to clarify the effect of exogenously applied LM-332 on wounds of genetically diabetic db/db mice. We studied wound healing after application of both soluble LM-332 and an engineered LM-332 biomaterial.

METHODS

Animals and Wounding

Genetically diabetic 8-12 week old male mice (db/db; C57BL/Ks J-*m*+/+ Lepr^{db}) and non diabetic db/- littermates were purchased (The Jackson Laboratory, Bar Harbor, ME) and housed individually in the University of Washington Department of Comparative Medicine vivarium, maintained on a 12 hour light-dark cycle and allowed *ad libitum* access to rodent chow and water. Strain and age of mouse were chosen because the mutant mice exhibit severe diabetic conditions with plasma insulin concentration and hyperglycemia peaking between 8-12 weeks (9,38). Fifteen db/db and fifteen db/- mice were used to evaluate LM-332 protein expression and immunohistochemistry of untreated wounds. Twenty-nine db/db mice were used for LM-332 topical application studies.

Mice were anesthetized with an intraperitoneal injection (IP) of ketamine (150 mg/ml) and xylazine (10 mg/ml) (Phoenix Pharmaceuticals Inc.; St. Joseph, MO). The dorsal skin was shaved, treated with depilatory cream and cleansed with povidine-iodine solution. Mice were kept warm during anesthesia and surgery using a heat lamp and heating pad maintained at approximately 38°C. Four full thickness 6-mm punch biopsies (Acuderm Inc., Ft. Lauderdale, FL) were created on the dorsal surface of the mice (4). Depending on experimental goals, wounds were next covered with Tegaderm™ (3M, St. Paul, Minn.) or a combination of biomaterial beneath a covering of Tegaderm™ for LM-332 delivery studies. The mice tolerated the anesthesia, wounding procedure and application of soluble reagents without problems. Mice did not experience large weight change during the study and 90% survived the anesthesia and experiments. All animal studies were conducted with University of Washington Animal Care Committee approval.

Basement Membrane Protein Expression and Immunohistochemistry in Untreated db/db and db/- Wounds

Mice were euthanized with an IP injection of sodium pentobarbital (210mg/kg) (Abbot Laboratories; North Chicago, IL) for tissue harvest. Tissue sections of unwounded skin and wounds, with surrounding tissue (approximately 0.5cm), were harvested at 1, 3, 7, 10, 14 days post-wounding. Tissue was frozen in O.C, T, (Sakura FineTek, Torrance, CA) and sectioned for immunohistochemistry.

Six to eight micron tissue sections were either treated with 1% Triton and fixed with 2% formaldehyde, treated with 2% Triton-PBS and fixed with 10% acetic acid, 15% methanol, or fixed with cold acetone. Standard indirect horseradish peroxidase immunohistochemistry was used with 3,3'-diaminobenzidine as a chromogen was used to evaluate basement membrane protein expression. Primary antibodies included integrin α6 (1:750, rat monoclonal G0H3), integrin β4 [1:2000, rat monoclonal, Pharmingen (BD Biosciences, San Jose, CA)], BP 230 [1:250, Dr. Takahashi Hashimoto (39)], Type VII collagen [1:14,000, Dr. David Woodley and Dr. Mei Chen (40)], precursor α chain of LM-332 [1:25, Dr. William Carter (32)], and cleaved α chain of LM-332 [1:10, Dr. William Carter (32)]. Secondary antibodies included biotinylated goat anti-rabbit IgG (1:300), biotinylated goat anti-human IgG (1:200) and biotinylated rabbit anti-rat IgG (1:200) (Vector Laboratories Inc., Burlingame, CA).

LM-332 Partial Purification for Application to Mouse Wounds

Primary KCs from normal human foreskins (HFKs) were grown as described previously (41) in serum-free KC growth medium (KGM; Clonetics, Corp., San Diego, CA) containing insulin, epidermal growth factor, hydrocortisone, and bovine pituitary extract (50μg protein/mL). Conditioned culture medium from confluent cultures of HFKs was passed over gelatin sepharose to remove fibronectin. LM-332 was removed from the medium on the final column

by adherence to wheat germ agglutinin (33). The result of this process was a partially purified form of soluble LM-332 with a protein content of 65μg/mL.

The functional activity of LM-332 was tested by an adhesion assay with HFKs. Microtiter 24-well plates were incubated with 25μL of serial dilutions of LM-332. The plates were seeded with 0.1 mL of suspended calcein labeled HFKs at a concentration of 5×10^6 HFKs per mL, which were allowed to adhere for 20 minutes at room temperature (RT). Fluorescence of the wells was read before and after three washes with phosphate buffered saline (PBS) to determine the fraction of HFKs that adhered to the LM-332 coated plate.

C2-5 Antibody Purification

C2-5 is a mouse anti-human monoclonal antibody directed against the amino terminal of the α3 chain of human LM-332 and does not cross react with mouse LM-322. C2-5 was purified through passage of hybridoma culture supernatant over a protein G-Sepharose column as previously described (18,24).

LM-332 Biomaterial

LM-332 was immobilized onto Tegaderm™ (3M, St. Paul, Minn.) to form a biomaterial. Tegaderm™ is a semi-occlusive dressing commonly used to cover wounds. Tegaderm™ used to form these biomaterials did not have an adhesive surface and was provided by the manufacturer. Tegaderm™ was cut into 1 cm squares, placed in 24-well Petri plates and incubated with 250μL of the monoclonal antibody C2-5 (10μg/mL) at 4°C for 24 h. The C2-5 coated Tegaderm™ (C2-5 biomaterial) was rinsed three times with PBS then blocked with sterile heat-denatured BSA (5 mg/ml in PBS) at 4°C for 24 h. The C2-5 biomaterial was then incubated with 200μL of LM-332 (10 μg/ml) at 4°C for 24 h. The affinity of C2-5 for the amino terminal of the α3 chain of LM-332 (Figure 1) immobilizes LM-332 on the C2-5 biomaterial by antibody trapping (42) to form a LM-332 biomaterial. C2-5 bound to LM-332 induces keratinocyte adhesion, spreading, and phosphorylation of focal adhesion kinases (42). The LM-332 biomaterial was rinsed three times with PBS then blocked with sterile heat-denatured BSA (5 mg/ml in PBS) at 4°C for 24 h. Presence of C2-5 and C2-5/ LM-332 on Tegaderm™ was confirmed by immunostaining.

The functional activity of the LM-332 biomaterial was tested by an adhesion assay with HFKs. While HFKs were used for adhesion assays, human LM-332 has been shown to have an important role in regulating tissue organization, gene expression, and survival of mouse epidermal keratinocytes as well (25). The LM-332 biomaterial and controls were placed in 24-well Petri plates. Controls were the non-adhesive Tegaderm ™ and the C2-5 biomaterial. The LM-332 biomaterial and controls were seeded with 0.1 mL of suspended HFKs at a concentration of 5×10^6 HFKs per mL, which were allowed to adhere for 20 minutes at RT. The LM-332 biomaterial and controls were then washed three times with PBS, fixed for 20 min with 2% formaldehyde, and stained with Coomassie blue. The excess dye was washed off with PBS and biomaterials were examined with light microscopy to evaluate HFK adhesion.

Determining Dosing Schedule of Soluble LM-332 to Mouse Wounds

Before studies to test the effects of LM-332 on wound healing, a dosing schedule was determined by evaluating for the presence of LM-332 in the mouse wound environment after a single topical application. To permit detection by fluorescence after application, LM-332 was conjugated with NHS-LC-Biotin (biotinylated LM-332) using EZ Link™ (Pierce Chemical Company, Rockford, IL) according to manufacturer's protocol. Two animals were used to evaluate the presence of biotinylated LM-332 at one and 24 hours after a single application. Two wounds on each mouse were treated with biotinylated LM-332 and two wounds were treated with saline as a control. The mice were euthanized at 1 and 24 hours. Dorsal mouse

skin including all four wounds was removed *en bloc*. Tissue was fixed in 4% paraformaldehyde at 4°C for 10 minutes. Tissue was then rinsed in tris-buffered saline (TBS) and blocked in 2% goat serum for 1 hour. The *en face* wound beds were next incubated with streptavidin-Cy5 (1:500 dilution; Jackson Immuno Research Laboratories, West Grove, PA), at RT for 30 minutes then rinsed in TBS at 4°C overnight. Nuclei were stained with 4', 6-diamidino-2-phenylindole (DAPI) (Sigma Chemical Co., St. Louis, MO.) for 5 minutes at RT. The wounds were mounted in an anti-quench medium containing n-Propyl Gallate for epi-fluorescence microscopy. The wound beds were first imaged with differential interference contrast (DIC) to identify and focus on the dorsal surface followed by epi-fluorescence illumination to record the Cy5 fluorescence signal. Signal was detectable on mouse wounds at both one and 24 hours after a single application. No signal was seen on mouse wounds treated with saline control (Figure 2). Because LM-332 was still detectable on wound beds for at least 24 hours, a single daily dose of LM-332 was administered for 7 days.

LM-332 Delivery to Wounds

Four wounds were created on the backs of each mouse and each wound received one of four treatments (soluble LM-332, PBS as a soluble control, LM-332 biomaterial, or C2-5 biomaterial as a control). We applied each treatment to cranial (anterior) wounds in some mice and caudal (posterior) wounds in others because cranial-caudal differences in wound healing have been observed (43).

Soluble LM-332: Soluble LM-332 or PBS, as a control, was delivered to one of the anterior of the four wounds on 20 mice and to one of the posterior wounds on 7 mice (Figure 3). Treatment solutions (0.1 ml) were infused between the Tegaderm™ and wound using a syringe and 30-gauge needle. Soluble LM-332 delivered to one of four wounds on the dorsal surface of the db/db mouse with this method does not spread to adjacent wounds(4). A single, daily dose of soluble LM-332 was administered to wounds for 7 days post-wounding.

LM-332 biomaterial: LM-332 biomaterial or C2-5 biomaterial, as a control, was placed on wounds. The LM-332 biomaterial was applied to one of the anterior wounds on 7 mice and to the posterior wound on 20 mice. The C2-5 biomaterial was applied to one of the anterior wounds on 7 mice and to one of the posterior wounds on 8 mice.

Wound Closure

Wounds were photographed on days 0, 7 and 14 using a Nikon D1 digital camera equipped with a Micro Nikkor macro lens and dual electronic flash. Polarizing filters were fitted over both the flash and lens. Cross polarization of these filters was found to be essential to remove spectral reflections from the Tegaderm™ or wound surface. A ruler was included in each image for spatial calibration. Three independent readers evaluated wounds for percent closure. Covered wounds could be visualized through the translucent Tegaderm™. Adobe Photoshop® 5.0 (Adobe; San Jose, CA) software loaded with the Image Processing Tool Kit 2.5 (Reindeer Games; Asheville, NC) was used to analyze wound closure and wound bed Cy5 fluorescence signal. The wound area was determined by opening the image in Photoshop®, spatially calibrating the image using the scale bar, demarcating the wound edge, filling the interior with black and measuring this area in square mm. Wound areas on day 0 were used as a reference and % wound closed was calculated for subsequent time points (7).

Wound Harvesting

Mice were euthanized 14 days after wounding. To permit fair comparison, all wounds remained covered with Tegaderm™ throughout the duration of the study (4). Dorsal mouse skin, including all 4 wounds and a 0.5 cm margin of unwounded skin, was removed *en bloc* and fixed in 10% neutral buffered formalin (NBF) or frozen in O.C.T (Sakura Finetek USA, CA).

Following fixation, the dorsal skin was stained with hematoxylin for 5 minutes to demarcate the central area of the wound that had not yet epithelized. Photographs of wounds were obtained and then wounds were bisected in a sagittal plane through the widest margin of the wound. Following fixation, tissue was rinsed in PBS, dehydrated through graded alcohol, and embedded in paraffin so the mid-portion of the wound could be sectioned for routine hematoxylin and eosin (H & E) histological evaluation.

Wound Histology

Photomicrography was performed using a Nikon Microphot SA microscope with differential interference contrast and epi-fluorescence illumination equipped with a Photometrics Sensys Monochrome digital camera controlled by IP Lab® software (Scanalytics, Vienna, VA). H & E stained wound sections were imaged using brightfield illumination. Individual grayscale images captured through red, green and blue separation filters were merged and saved as 24-bit color image files. Tissue sections were visualized by three investigators and given a score ranging from 1 to 12, with 1 representing no healing and 12 representing complete closure and advanced dermal repair using scoring methods previously published (7,44). Briefly, sections were scored based on dermal cell invasion, granulation tissue formation, vascularity and extent of epithelization.

Data Analysis

Correlation of % wound closed and histology scores of the three readers were evaluated with Spearman's test. If significant correlation was found then scores of the three readers were combined and averaged for subsequent analysis. The Wilcoxon rank-sum test was used to test for potential differences in the size of day zero wounds between anterior and posterior wounds with wound used as the unit of analysis. We used the Kruskal-Wallis test followed by the Wilcoxon rank-sum test for multiple comparisons to evaluate for potential differences in histology scores and % wound closed between wounds treated with soluble LM-332, PBS, LM-332 biomaterial or C2-5 biomaterial with wound used as the unit of analysis. Results were corrected for multiple comparisons between wound treatments using Bonferroni's method. A P value of less than 0.05 indicates statistical significance. All analysis was done with Stata Statistical Software 8.0 (StataCorp, College Station, TX).

RESULTS

Evaluation of Basement Membrane Components in db/db and db/- Mouse Wounds

Integrin α6, β4, BP230, type VII collagen and cleaved LM-332 were expressed along the basement membrane in all of the 1 to 14 day wounds. There were no appreciable differences between db/db and db/- mouse wounds for expression for these proteins (data not shown). Precursor LM-332 was expressed in leading edge KCs in both db/db and db/- wounds up to 3 days (Figure 4A and B). However, precursor LM-332 expression in the leading edge keratinocytes was markedly reduced after 7 days for db/db mice wounds (Figure 4D and F) as compared to db/- littermates (Figure 4C and E). The day 14 db/- wounds were all closed with no residual immunohistochemical evidence for precursor LM-332 (data not shown).

Partially Purified LM-332 Functional Activity

LM-332 functional activity was confirmed *in vitro* by adhesion assays with HFKs. Adhesion assays with serial dilutions of LM-332 demonstrated optimal adhesion of HFKs at a concentration of 65 μg/mL, which was 10X that necessary for significant HFK adhesion. Given this functional activity, LM-332 at a concentration of 65 μg/mL was used for our subsequent studies involving topical application of soluble LM-332. Adhesion assays with the LM-332

biomaterial also demonstrated adhesion of a relatively high number of HFKs, while few cells adhered to the control biomaterials (Figure 5).

Wound closure

Wounds created on db/db mice with biopsy punch were quite reproducible with a mean area of 29.7 ± 3.8 mm^2 immediately following wounding. Wounds enlarged after excision and became 5.3% larger than the punch biopsy instrument. No significant difference in initial wound area was found when the four wounds from all mice, cranial and caudal, were compared ($p=0.42$).

Three readers independently measured the area of wounds on day 0, 7 and 14 for all wounds. Correlation of % wound closed was statistically significant at each time point between investigators (day 0: $r=0.92$ to 0.96, $p<0.001$, day 7: $r=0.71$ to 0.82, $p<0.001$, day 14: $r=0.68$ to 0.73, $p<0.001$). Therefore, measurements of the three investigators were combined and averaged for all subsequent wound closure analysis.

The db/db mouse wounds had limited % closed at day 7 and were not yet closed at day 14. No statistically significant differences in % wound closed were found at either day 7 or 14 for any of the treatment groups ($p=0.10$ at day 7, $p=0.52$ at day 14) (Figure 6).

We have previously demonstrated that gross examination of wounds through Tegaderm™ interferes with % wound closed evaluation. (4). Therefore, after wound area and % wound closed were calculated on day 14 *in situ*, the wounds were harvested, the Tegaderm™ removed, the wounds were fixed in formalin and then stained *en bloc* with hematoxylin. Wound area and % wound closed of these day 14 hematoxylin stained wounds were then re-calculated. Correlation between investigators of % wound closed of day 14 hematoxylin stained wounds was statitistically significant ($r=0.61$ to 0.67, $p<0.001$). The measured % wound closed of day 14 hematoxylin stained wounds was compared to the *in situ* measured % wound closed of day 14 wounds. The day 14 hematoxylin stained wounds were found to have a significantly greater % wound closed (69.6 ± 18.1 vs. 45.1 ± 18.5, $p<0.001$). Tegaderm™ removal along with hematoxylin staining aids in % wound closed evaluation (Figure 7). No statistically significant differences in % wound closed were found between day 14 hematoxylin stained wounds for any of the treatment groups ($p=0.28$).

Wound Histology

Wounds treated for the first 7 days after wounding with soluble LM-332, PBS or a single application of a LM-332 or C2-5 biomaterial were harvested on day 14. Histological examination showed a consistent wound depth through the panniculus carnosus and varying degrees of wound healing as measured by cell invasion, granulation tissue, vascularity and epithelization. Three investigators independently scored the histology of the wounds and correlation between investigators was significant ($r=0.80$ to 0.93, $p<0.001$). Because investigators measurements were highly correlated, they were combined and averaged for all subsequent histology score analysis.

Wounds treated with soluble LM-332 had the highest histology score (Figure 8). However, when individual comparisons between wound treatments were performed and corrected for multiple comparisons using Bonferroni's method, no significant differences were found ($p>0.05$).

DISCUSSION

The db/db mouse has diabetes mellitus symptoms, including impaired wound healing (7,38). Additionally they have decreased epidermal nerve counts compared to non-diabetic littermates

and markedly increased levels of neutral endopeptidase (NEP), the enzyme which degrades substance P (45). The increased NEP levels are similar to those observed in diabetic humans (46). The db/db mouse, therefore, has been used as a wound healing model for type 2 diabetes mellitus (4,7). We have demonstrated that in human diabetic chronic wounds, KCs proliferate at the wound edge, but fail to migrate (11). KC migration and anchorage are mediated by LM-332. We proposed that defective LM-332 mediated KC migration contributes to healing failure and LM-332 application may enhance diabetic wound healing.

We first evaluated basement membrane protein expression in diabetic db/db and normal db/- mouse 1 to 14 day wounds. We found that precursor LM-332 was markedly reduced in the migrating epithelial tongue in the 7 to 14 day db/db wounds as compared to db/- littermates. This reduction in precursor LM-332 was similar to that seen in human chronic wounds when compared with normal acute wounds (Usui ML, et al. submitted). The paucity of LM-332 in the db/db mouse then served as rationale for use of the db/db mouse model for our studies.

The wound model employed in this study has been validated using a 6 mm biopsy punch to create four wounds on a db/db mouse (4). Two wounds were treated with soluble LM-332 or PBS control in the db/db mice. The LM-332 was partially purified from HFK cell culture supernatant and shown to be functional *in vitro* by HFK adhesion studies. The other 2 wounds were covered with the C2-5 biomaterial or the LM-332 biomaterial. An advantage of using C2-5 as a first step in making the LM-332 biomaterial is C2-5 selective affinity for the LM-332 amino terminal portion of the α chain. This step further purifies the LM-332 on the biomaterial and orients the active carboxy terminal portion of the α chain towards the wound. This antibody trapping (42) immobilization strategy for attaching LM-332 onto the C2-5 coated Tegaderm™ promoted HFK adhesion *in vitro*. These biomaterials and the immobilization methods described in this paper may also serve an important role in allowing KC attachment to percutaneous devices such as vascular access catheters.

While the Tegaderm™ was valuable as a LM-332 carrier, transparency reduced with time and wound evaluation was obscured. As with our previous study (4), calculation of % wound healed based on visual observation was significantly altered for wounds covered with Tegaderm™ when compared to more direct measurements. Tegaderm™ removal after wound harvesting and staining wound beds with hematoxylin allowed more accurate assessment of % wound healed since hematoxylin has nuclear affinity and stains the cellular invasion and granulation tissue of the central portion of the wound that had not yet epithelized. Wound healing assessment must be accurate if the effects of therapeutic interventions such as LM-332 are to be determined.

Neither daily topical application of soluble LM-332 for 7 days, nor a single application of a LM-332 biomaterial increased the % wound healed at 7 and 14 days compared to control treatments. For these experiments we used LM-332 partially purified from HFKs. The partially purified LM-332 may also contain KC products that could contribute to wound closure separate from that of LM-332. More complete purification of LM-332 from HFKs is also possible, but results in an insoluble form of the glycoprotein. Maintaining the soluble nature of LM-332 is necessary for topical application to wounds. Additionally, the LM-332 contains a mix of both the precursor LM-332 as well as the cleaved LM-332. We have previously reported that Western blots indicated that the protein was primarily the cleaved LM-332 with only small amounts of precursor LM-332 (32). In normal human acute wounds, both precursor LM-332 and its mRNA have been detected in migrating KCs for up to 7 days. In chronic human diabetic wounds, precursor LM-332 mRNA is generally absent, and the precursor LM-332 protein is detected only sporadically. Cleaved LM-332 can be detected in both normal and diabetic wounds of humans (Usui ML, et al. submitted).

Perhaps the failure to speed wound closure using exogenously applied LM-332 was because the LM-332 applied was primarily the cleaved LM-332 form. Cleaved LM-332 has been shown to enhance hemidesmosome assembly with integrin α6β4 and act as an adhesive factor that retards cell migration (28,47). Presence of cleaved LM-332 may have promoted KC adhesion and reduced any potential effect on KC migration and wound healing. Therefore, the cleaved LM-332 isolated from HFKs may not be the isomer of greatest interest to stimulate wound healing. In the future, similar studies using full length precursor LM-332 could be performed. Unfortunately, soluble purified precursor LM-332 is not currently available and when present even in small quantity, may be quickly cleaved (32). Sigle et al. 2004 have engineered and expressed a non-cleavable LM-332 molecule by eliminating the cleavage site between the G4/G5 segment and the remainder of the α chain (32). This approach bypasses the issue of rapid cleavage of LM-332, but this genetically engineered molecule is almost completely deposited by the KC's, precluding its release to culture medium and collection in sufficient quantities to test on experimental wounds. It is also possible the that the KCs must make and deposit LM-332 onto the ECM in order for migration to proceed and that strategies directed at enhanced LM-332 expression by wound KCs rather than exogenous application of LM-332 isoforms to the wound would be more successful.

LM-332 did not promote wound healing at the microscopic level as measured by histology scores of cell invasion, granulation tissue formation, neovascularization and epithelization at day 14. When all wounds were compared, including those treated with soluble LM-332, PBS, LM-332 biomaterial and the C2-5 biomaterial, the LM-332 treated wounds were found to have a higher histology score. However, after statistical correction for multiple comparisons, no statistically significant differences were found. Perhaps a larger sample size would permit detection of a significant difference, but we have concluded that any enhanced healing response in this study was moderate at best and not likely to be clinically important.

Chronic non-healing wounds in patients with diabetes mellitus results in significant morbidity and an increased risk for amputation. LM-332 most likely plays a role in the impaired KC migration and delayed healing seen in diabetic wounds. However, topical application of cleaved LM-332 in both a soluble form and as a biomaterial did not improve wound healing in this study. Precursor LM-332 may play a more prominent role in KC migration and wound healing. If strategies can be developed to induce KCs at the wound margin to produce more native precursor LM-332 or an uncleavable form of precursor LM-332, this role can be tested.

Acknowledgements

This work was supported by NIH awards R01 AR43006, R01 DK58007 and R01 GM56483, NSF EEC 9529161 [University of Washington Engineered Biomaterials (UWEB)], the George F. Odland Endowed Research Fund and a University of Washington Warren G. Magnuson Scholarship.

References

1. Pecoraro RE, Reiber GE, Burgess EM. Pathways to diabetic limb amputation. Basis for prevention. Diabetes Care 1990;13(5):513–21. [PubMed: 2351029]
2. Reiber GE. The epidemiology of diabetic foot problems. Diabet Med 1996;13(Suppl 1):S6–11. [PubMed: 8741821]
3. American Diabetes Association. Consensus Development Conference on Diabetic Foot Wound Care. Diabet Care 1999;22(8):1354–60.
4. Sullivan S, Underwood R, Gibran N, Sigle RO, Usui M, Carter WG, O JE. Validation of a model for the study of multiple wounds in the diabetic mouse (db/db). Plast Reconstr Surg 2004;113(3):953–960. [PubMed: 15108888]
5. Tsuboi R, Shi CM, Rifkin DB, Ogawa H. A wound healing model using healing-impaired diabetic mice. J Dermatol 1992;19(11):673–5. [PubMed: 1293153]

6. Ring BD, Scully S, Davis CR, Baker MB, Cullen MJ, Pelleymounter MA, Danilenko DM. Systemically and topically administered leptin both accelerate wound healing in diabetic ob/ob mice. Endocrinology 2000;141(1):446–9. [PubMed: 10614668]
7. Greenhalgh DG, Sprugel KH, Murray MJ, Ross R. PDGF and FGF stimulate wound healing in the genetically diabetic mouse. Am J Pathol 1990;136(6):1235–46. [PubMed: 2356856]
8. Debray-Sachs M, Dardenne M, Sai P, Savino W, Quiniou MC, Boillot D, Gepts W, Assan R. Anti-islet immunity and thymic dysfunction in the mutant diabetic C57BL/KsJ db/db mouse. Diabetes 1983;32(11):1048–54. [PubMed: 6357903]
9. Coleman DL. Obese and diabetes: two mutant genes causing diabetes-obesity syndromes in mice. Diabetologia 1978;14(3):141–8. [PubMed: 350680]
10. Mordes JP, Rossini AA. Animal models of diabetes. Am J Med 1981;70(2):353–60. [PubMed: 6451172]
11. Olerud JE, Usui ML, Muffley LA, Smith DG, Larsen JA, Gibran NS, Mansbridge JN, Carter WG. Epithelial cells in the wound margins of diabetic ulcers are highly proliferative. J Invest Dermatol 2000;114(4):857.
12. Andriessen MP, van Bergen BH, Spruijt KI, Go IH, Schalkwijk J, van de Kerkhof PC. Epidermal proliferation is not impaired in chronic venous ulcers. Acta Derm Venereol 1995;75(6):459–62. [PubMed: 8651025]
13. Stenn, KS.; dePalma, L. Re-epithelialization. In: Clark, RAF.; Henson, PM., editors. The Molecular and Cellular Biology of Wound Repair. New York: Plenum Press; 1988. p. 321-335.
14. Zhang K, Kramer RH. Laminin 5 deposition promotes keratinocyte motility. Exp Cell Res 1996;227 (2):309–22. [PubMed: 8831569]
15. Carter WG, Ryan MC, Gahr PJ. Epiligrin, a new cell adhesion ligand for integrin alpha 3 beta 1 in epithelial basement membranes. Cell 1991;65(4):599–610. [PubMed: 2032285]
16. Vailly J, Verrando P, Champliaud MF, Gerecke D, Wagman DW, Baudoin C, Aberdam D, Burgeson R, Bauer E, Ortonne JP. The 100-kDa chain of nicein/kalinin is a laminin B2 chain variant. Eur J Biochem 1994;219(12):209–18. [PubMed: 8306988]
17. Rousselle P, Lunstrum GP, Keene DR, Burgeson RE. Kalinin: an epithelium-specific basement membrane adhesion molecule that is a component of anchoring filaments. J Cell Biol 1991;114(3): 567–76. [PubMed: 1860885]
18. Nguyen BP, Ren XD, Schwartz MA, Carter WG. Ligation of integrin alpha 3beta 1 by laminin 5 at the wound edge activates Rho-dependent adhesion of leading keratinocytes on collagen. J Biol Chem 2001;276(47):43860–70. [PubMed: 11571278]
19. Watt FM. Role of integrins in regulating epidermal adhesion, growth and differentiation. Embo J 2002;21(15):3919–26. [PubMed: 12145193]
20. Goldfinger LE, Hopkinson SB, deHart GW, Collawn S, Couchman JR, Jones JC. The alpha3 laminin subunit, alpha6beta4 and alpha3beta1 integrin coordinately regulate wound healing in cultured epithelial cells and in the skin. J Cell Sci 1999;112(Pt 16):2615–29. [PubMed: 10413670]
21. Hintermann E, Bilban M, Sharabi A, Quaranta V. Inhibitory role of alpha 6 beta 4-associated erbB-2 and phosphoinositide 3-kinase in keratinocyte haptotactic migration dependent on alpha 3 beta 1 integrin. J Cell Biol 2001;153(3):465–78. [PubMed: 11331299]
22. Santoro MM, Gaudino G, Marchisio PC. The MSP receptor regulates alpha6beta4 and alpha3beta1 integrins via 14-3-3 proteins in keratinocyte migration. Dev Cell 2003;5(2):257–71. [PubMed: 12919677]
23. Xia Y, Gil SG, Carter WG. Anchorage mediated by integrin alpha6beta4 to laminin 5 (epiligrin) regulates tyrosine phosphorylation of a membrane-associated 80-kD protein. J Cell Biol 1996;132 (4):727–40. [PubMed: 8647901]
24. Gil SG, Brown TA, Carter RMC. Junctional epidermolysis bullosis: defects in expression of epiligrin/ nicein/kalinin and integrin beta 4 that ihibit hemidesmosome formation. J Invest Dermatol 1994;103 (5 Suppl):S31–38.
25. Ryan MC, Lee K, Miyashita Y, Carter WG. Targeted disruption of the LAMA3 gene in mice reveals abnormalities in survival and late stage differentiation of epithelial cells. J Cell Biol 1999;145(6): 1309–23. [PubMed: 10366601]

26. Frank DE, Carter WG. Laminin 5 deposition regulates keratinocyte polarization and persistent migration. J Cell Sci 2004;117(Pt 8):1351–63. [PubMed: 14996912]
27. Shang M, Koshikawa N, Schenk S, Quaranta V. The LG3 module of laminin-5 harbors a binding site for integrin alpha3beta1 that promotes cell adhesion, spreading, and migration. J Biol Chem 2001;276 (35):33045–53. [PubMed: 11395486]
28. O'Toole EA, Marinkovich MP, Hoeffler WK, Furthmayr H, Woodley DT. Laminin-5 inhibits human keratinocyte migration. Exp Cell Res 1997;233(2):330–9. [PubMed: 9194495]
29. Yamada, KM.; Clark, RA. Provisional Matrix. In: Clark, RA., editor. The molecular and cellular biology of wound repair. New York: Plenum Press; 1996. p. 51-82.
30. Burgeson RE, Chiquet M, Deutzmann R, Ekblom P, Engeln J, Kleinman H, Martin GR, Meneguzzi G, Paulsson M, Sanes J, et al. A new nomenclature for the laminins. Matrix Biol 1994;14(3):209–11. [PubMed: 7921537]
31. Goldfinger LE, Stack MS, Jones JC. Processing of laminin-5 and its functional consequences: role of plasmin and tissue-type plasminogen activator. J Cell Biol 1998;141(1):255–65. [PubMed: 9531563]
32. Sigle RO, Gil SG, Bhattacharya M, Ryan MC, Yang TM, Brown TA, Boutaud A, Miyashita Y, Olerud J, Carter WG. Globular domains 4/5 of the laminin alpha3 chain mediate deposition of precursor laminin 5. J Cell Sci 2004;117(Pt 19):4481–94. [PubMed: 15316072]
33. Carter WG, Kaur P, Gil SG, Gahr PJ, Wayner EA. Distinct functions for integrins alpha 3 beta 1 in focal adhesions and alpha 6 beta 4/bullous pemphigoid antigen in a new stable anchoring contact (SAC) of keratinocytes: relation to hemidesmosomes. J Cell Biol 1990;111(6 Pt 2):3141–54. [PubMed: 2269668]
34. Nguyen BP, Gil SG, Carter WG. Deposition of laminin 5 by keratinocytes regulates integrin adhesion and signaling. J Biol Chem 2000;275(41):31896–907. [PubMed: 10926936]
35. Matsui C, Wang CK, Nelson CF, Bauer EA, Hoeffler WK. The assembly of laminin-5 subunits. J Biol Chem 1995;270(40):23496–503. [PubMed: 7559513]
36. Marinkovich MP, Lunstrum GP, Keene DR, Burgeson RE. The dermal-epidermal junction of human skin contains a novel laminin variant. J Cell Biol 1992;119(3):695–703. [PubMed: 1383241]
37. Fujita M, Usui ML, Carter WG, Ryan MC, Olerud JE. Laminin 5 expression in acute and chronic wounds. J Invest Dermatol 1999;112(4):626.
38. Coleman DL. Diabetes-obesity syndromes in mice. Diabetes 1982;31(Suppl 1 Pt 2):1–6. [PubMed: 7160533]
39. Tanaka M, Hashimoto T, Dykes PJ, Nishikawa T. Clinical manifestations in 100 Japanese bullous pemphigoid cases in relation to autoantigen profiles. Clin Exp Dermatol 1996;21(1):23–7. [PubMed: 8689764]
40. Hessle H, Sakai LY, Hollister DW, Burgeson RE, Engvall E. Basement membrane diversity detected by monoclonal antibodies. Differentiation 1984;26(1):49–54. [PubMed: 6370774]
41. Boyce ST, Ham RG. Calcium-regulated differentiation of normal human epidermal keratinocytes in chemically defined clonal culture and serum-free serial culture. J Invest Dermatol 1983;81(1 Suppl): 33s–40s. [PubMed: 6345690]
42. Gil SG, Sigle RO, Carter WG. Detection and purification of instructive extracellular matrix components with monoclonal antibody technologies. Methods Cell Biol 2002;69:27–52. [PubMed: 12070998]
43. Martson M, Viljanto J, Laippala P, Saukko P. Cranio-caudal differences in granulation tissue formation: an experimental study in the rat. Wound Repair Regen 1999;7(2):119–26. [PubMed: 10231513]
44. Crowe MJ, McNeill RB, Schlemm DJ, Greenhalgh DG, Keller SJ. Topical application of yeast extract accelerates the wound healing of diabetic mice. J Burn Care Rehabil 1999;20(2):155–62. [PubMed: 10188114]
45. Spenny ML, Muangman P, Sullivan SR, Bunnett NW, Ansel JC, Olerud JE, Gibran NS. Neutral endopeptidase inhibition in diabetic wound repair. Wound Repair Regen 2002;10(5):295–301. [PubMed: 12406165]

46. Antezana M, Sullivan S, Usui M, Gibran N, Spenny M, Larsen J, Ansel J, Bunnett N, Olerud J. Neutral endopeptidase activity is increased in the skin of subjects with diabetic ulcers. J Invest Dermatol 2002;119(6):1400–4. [PubMed: 12485446]

47. Baker SE, Hopkinson SB, Fitchmun M, Andreason GL, Frasier F, Plopper G, Quaranta V, Jones JC. Laminin-5 and hemidesmosomes: role of the alpha 3 chain subunit in hemidesmosome stability and assembly. J Cell Sci 1996;109(Pt 10):2509–20. [PubMed: 8923212]

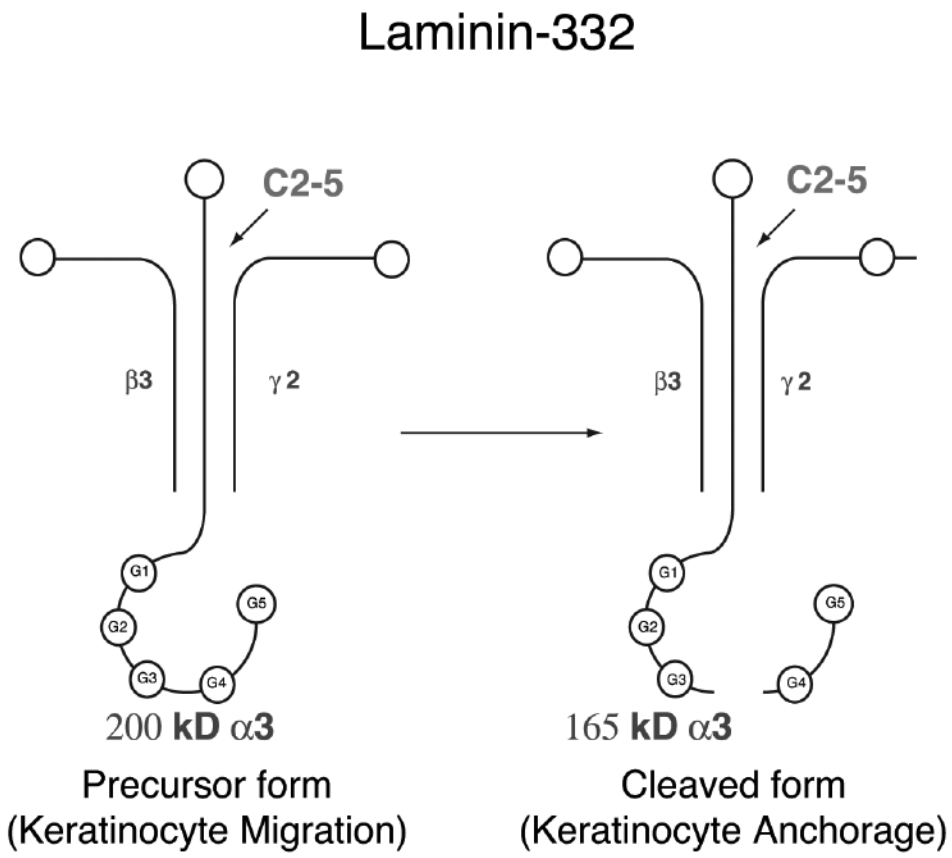

Figure 1.
LM-332 trimer with α3, β3 and γ2 subunits. The α chain of precursor LM-332 is cleaved at the G4/5 globular domains of the carboxy terminus to form cleaved LM-332. C2-5 antibody binds to the amino terminus of the α chain.

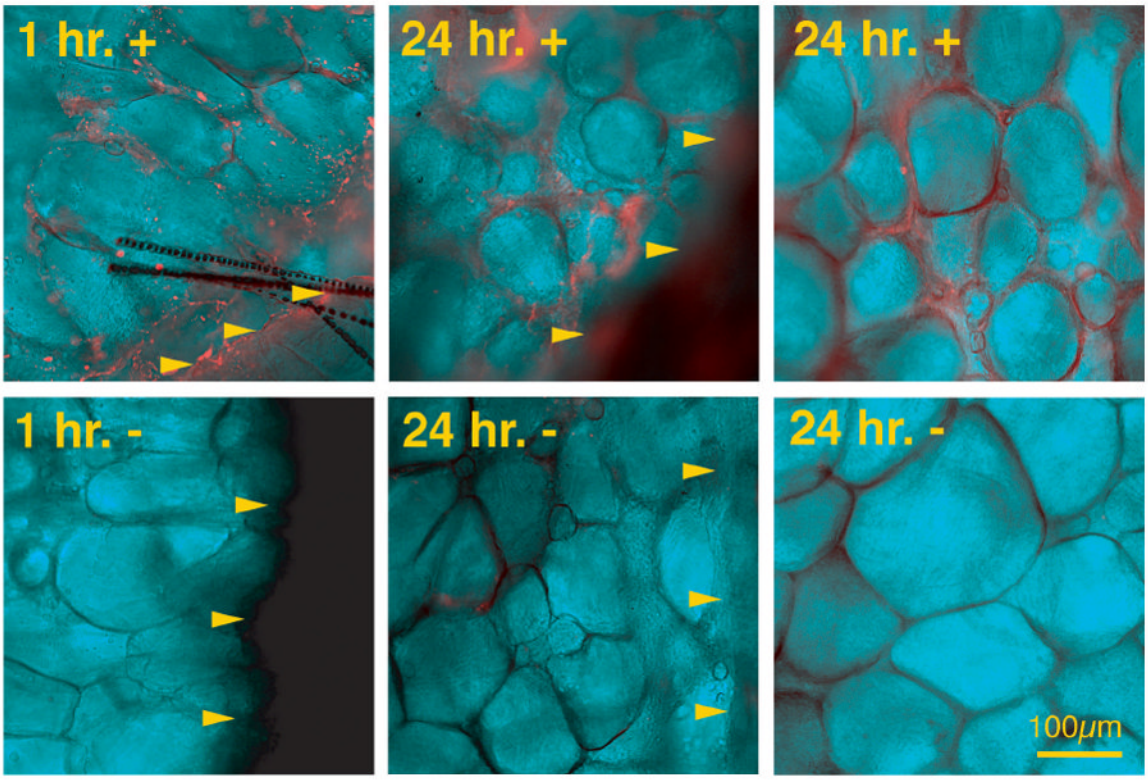

Figure 2.
Detection of LM-332 using immunofluorescence of whole mount wounds. Wounds treated with soluble biotinylated LM-332 and saline control at 1 and 24 hours. Arrowheads indicate wound margin. In soluble biotinylated LM-332 treated wounds, bright orange staining (fluorescent emission of streptavidin-Cy5) can be seen in the wound bed at both 1 and 24 hours after application, while immunofluorescence is absent in control wounds.

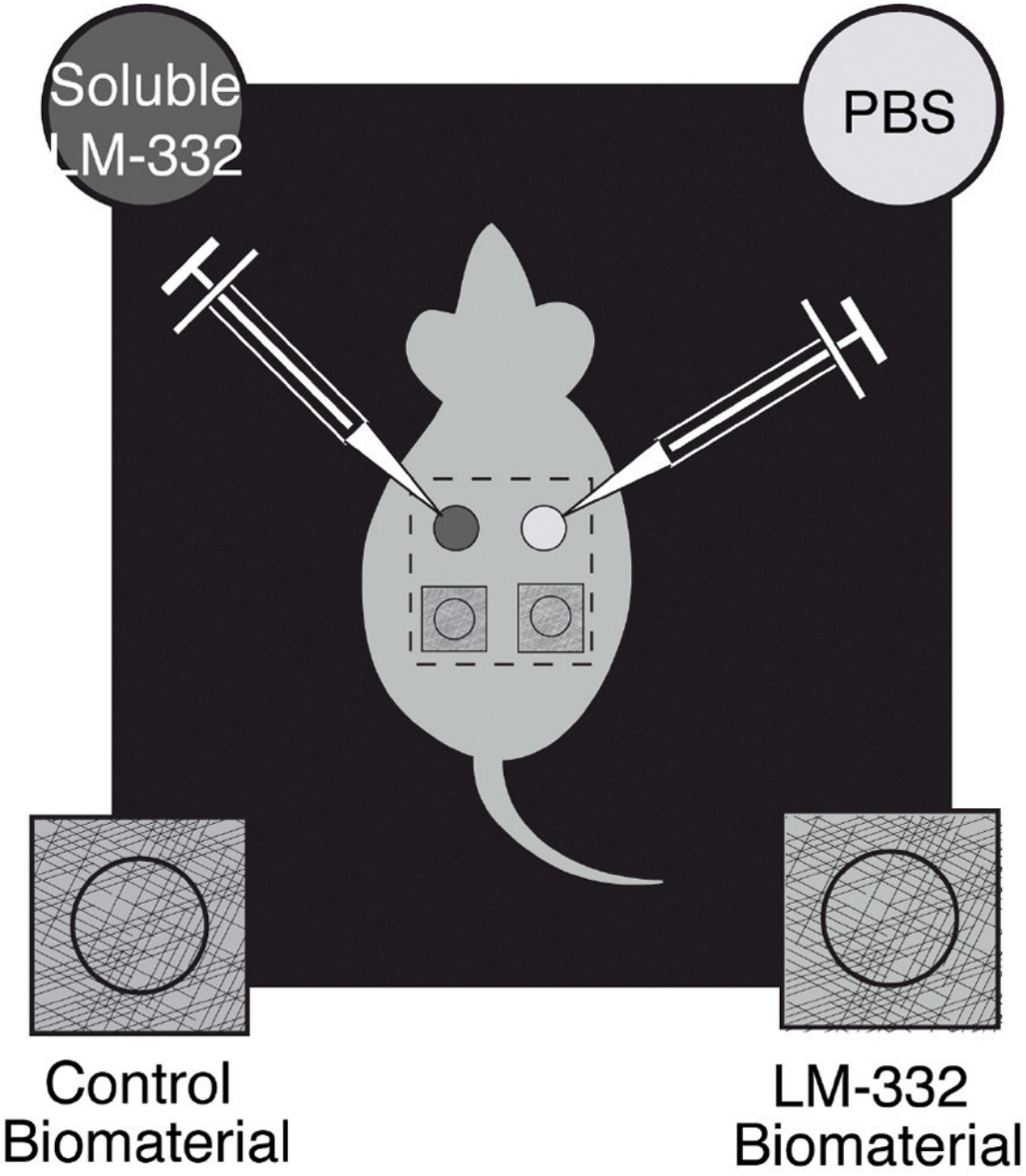

Figure 3.
Wounds treatments were soluble or biomaterials. Soluble wound treatments included LM-332 and phosphate buffered saline (PBS) as a control. Treatment solutions (0.1 ml) were infused beneath the Tegaderm™ using a syringe and 30-gauge needle. LM-332 biomaterial or C2-5 biomaterial as a control, was also delivered to wounds.

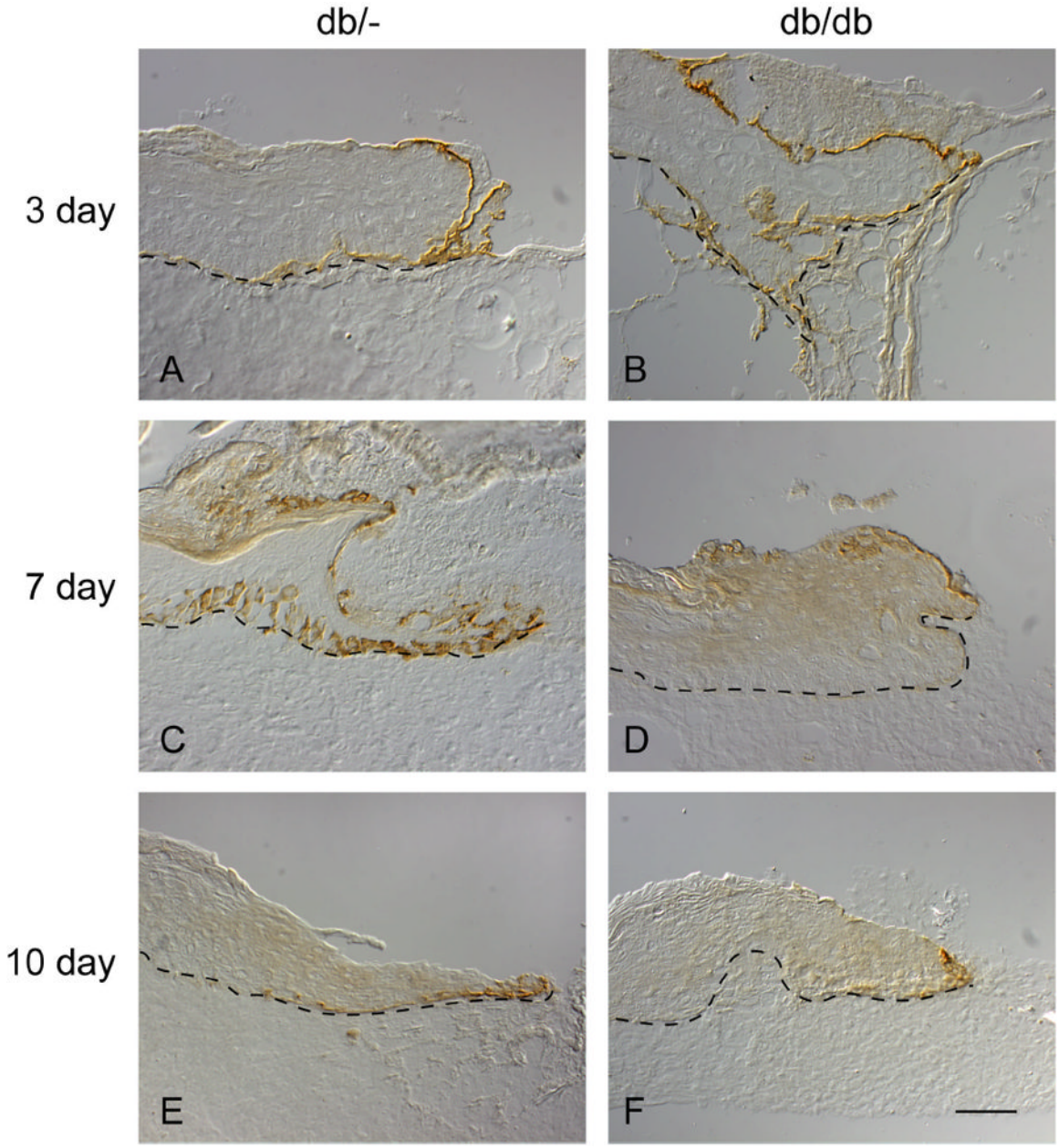

Figure 4.

Immunohistochemistry showing presence of precursor LM-332. Six millimeter punch wounds created on db/- (normal littermates) (Figures 4A, C and E) and db/db mice (Figures 4B, D and F) were harvested post-wounding at days 3 (Figures 4A and B), 7 (Figures 3C and D) and 10. Precursor LM-332 is present along the migrating epithelial wound tongue at 3 days for both the db/- and db/db mouse but is markedly reduced in the 7 day and 10 day db/db mouse wound (Figure 4D and F, respectively) as compared to their normal littermates (Figures 4C and E).

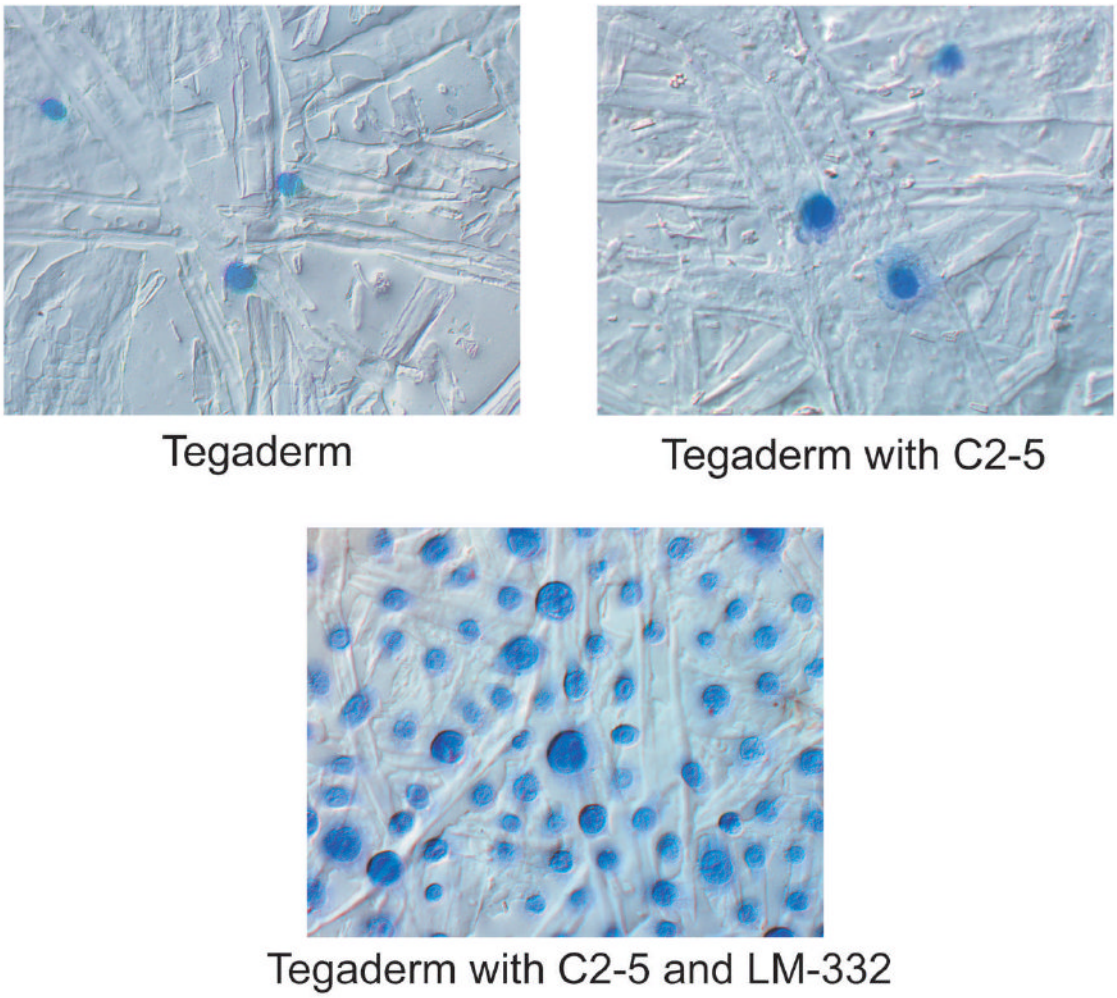

Figure 5.
Adhesion assay of human foreskin keratinocytes (HFKs) comparing Tegaderm™, Tegaderm™ coated with C2-5 antibody (C2-5 biomaterial) and Tegaderm™ coated first with C2-5 followed by LM-332 (LM-332 biomaterial). LM-332 biomaterial demonstrated adhesion of a relatively high number of HFKs, while few cells adhered to the control biomaterials (Tegaderm™ alone and C2-5 biomaterial).

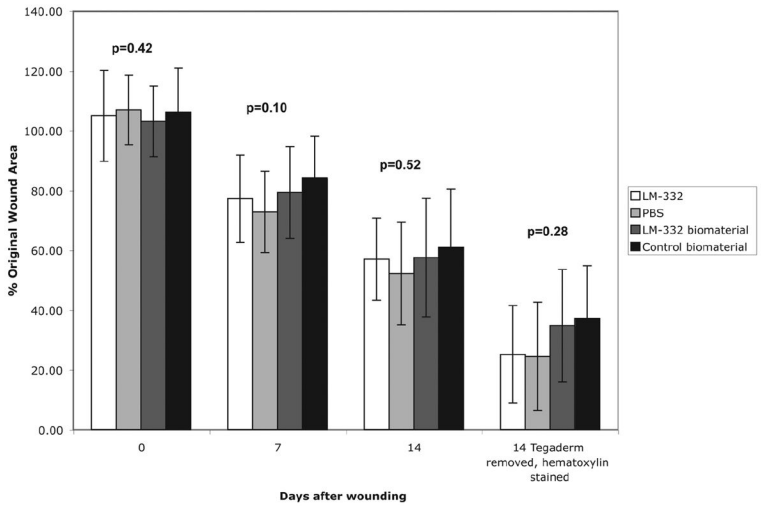

Figure 6.

Graph comparing % wound closed of LM-332, PBS, LM-332 biomaterial and C2-5 control biomaterial treated wounds at days 0, 7, 14 and at day 14 after removal of Tegaderm™ and hematoxylin staining. Wounds enlarged after excision, had limited % wound closed at day 7 and were not yet closed at day 14. No statistically significant differences in % wound closed were found at either day 7 or 14 between wounds treated with soluble LM-332 or PBS or wounds treated a LM-332 or C2-5 biomaterial (p=0.10 at day 7, p=0.52 at day 14).

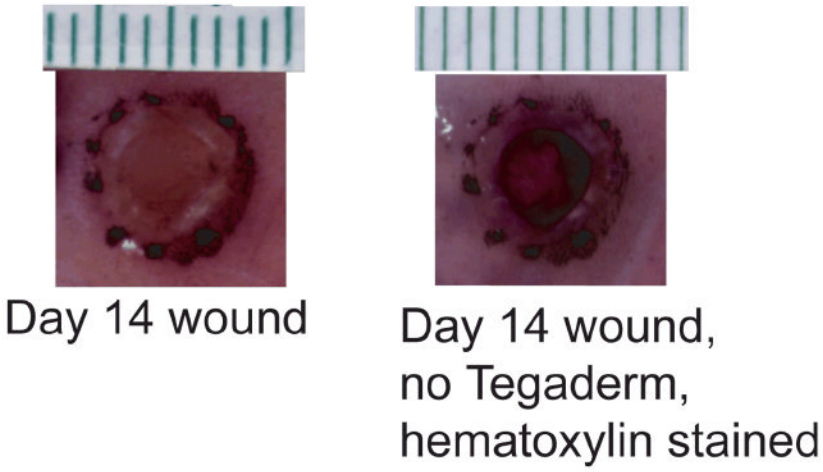

Figure 7.
Tegaderm™ covered wound at day 14 compared to the same wound with Tegaderm™ removed and stained with hematoxylin. Removal of Tegaderm™ and staining with hematoxylin aids in evaluation of the % wound closed.

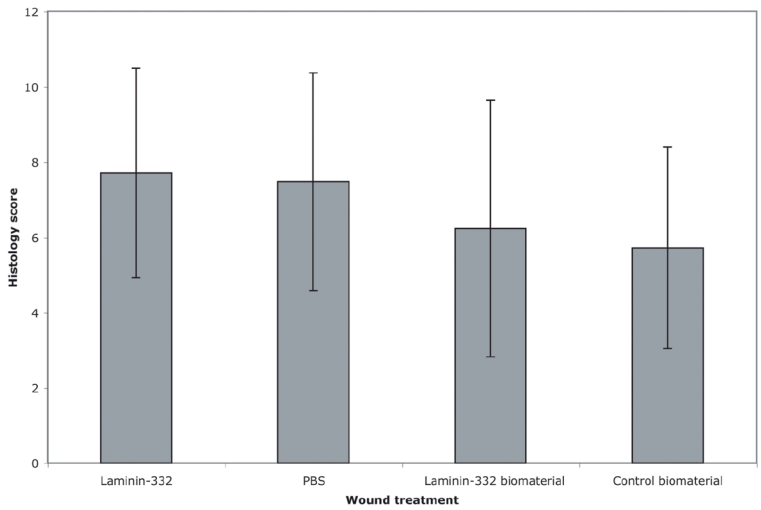

Figure 8.

Wound histology scores. Tissue sections were scored from 1 to 12, with 1 representing no healing and 12 representing complete closure. When individual comparisons were made between wound treatments, no significant differences were found between histology score based on wound treatment.